The (^{7}Li, ^{7}Beγ) reaction and isovector spin strength in ^{40}Ca

J. S. Winfield,* D. Beaumel, S. Galès, H. Laurent, I. Lhenry, and J. M. Maison
Institut de Physique Nucléaire, IN$_2$P$_3$-CNRS, 91406 Orsay Cedex, France

G. M. Crawley, S. Danczyk,† S. E. Hirzebruch,‡ J. C. Staško,§ and T. Suomijärvi‖
National Superconducting Cyclotron Laboratory, Michigan State University, East Lansing, Michigan 48824
(Received 19 January 1996)

The ^{40}Ca(^{7}Li, ^{7}Beγ) reaction at $E(^7\mathrm{Li})/A = 70$ MeV has been used to investigate isovector giant resonances and to measure the ratio of $\Delta S=1$ to $\Delta S=0$ spin strength in ^{40}Ca at high excitation energy. In the singles spectrum, the analogue of the giant dipole resonance is observed. Another resonance is observed at $E_x \approx 15$ MeV in the residual nucleus, which we suggest is a collective 2^- state. The isovector spin transfer strength at high excitation for the calcium target is compared to that measured with a carbon target under the same experimental conditions. Although more spin transfer strength at high excitation is observed for the calcium target than for the carbon target, this only accounts in part for an apparent discrepancy between previous ^{40}Ca($\vec{p},\vec{p}'$) and ^{12}C(^{7}Li, ^{7}Be) experiments. The general utility of the (^{7}Li, ^{7}Beγ) reaction is discussed. [S0556-2813(96)03807-1]

PACS number(s): 24.30.Cz, 25.70.Kk, 27.40.+z

I. INTRODUCTION

The study of simple modes of excitation such as giant resonances has been an abundant source of information about the nucleus. There are many data available on isoscalar ($\Delta T=0$) excitations from hadron and electron inelastic scattering, but it is only recently that isovector ($\Delta T=1$) modes of excitation have been studied beyond the well-known giant dipole and Gamow-Teller resonances. The spin response of the continuum at high excitation energy has been even less thoroughly investigated.

A particular problem has arisen recently concerning the nuclear spin excitation of the continuum. Glashausser *et al.* have measured inelastic proton scattering on ^{40}Ca with polarized protons at a bombarding energy of 319 MeV, and found that spin transfer ($\Delta S=1$) transitions are significantly enhanced compared to nonspin transfer ($\Delta S=0$) transitions at excitation energies between 20 and 40 MeV [1]. This enhancement can to a large extent be explained in terms of a model [2] of the response of a semi-infinite slab of interacting particles, and as such is not expected to be associated with a specific target. However, a subsequent measurement by Nakayama *et al.* of spin transfer strength for a ^{12}C target has found that at high excitation energies $\Delta S=0$ transitions are equal to, if not stronger than, $\Delta S=1$ transitions [3,4]. This latter experiment used the (^{7}Li, ^{7}Beγ) heavy-ion charge exchange reaction at $E/A = 26$ MeV. [The basis of the (^{7}Li, ^{7}Beγ) technique to separate spin transfer and nonspin transfer is described below.]

Although the (^{7}Li, ^{7}Be) result of Nakayama *et al.* is apparently in conflict with the ($\vec{p},\vec{p}'$) result of Glashausser *et al.*, several explanations are possible [3]. One hypothesis is that the ($\vec{p},\vec{p}'$) reaction may be dominated by isoscalar excitations, whereas (^{7}Li, ^{7}Be) is necessarily isovector. Another possibility is that while in the ($\vec{p},\vec{p}'$) case there is a dominant contribution to the continuum from quasifree charge exchange, in the heavy-ion reaction the contribution from this process may be small (see, e.g., Ref. [5]). Instead one might expect in the heavy-ion reaction continuum a contribution from three-body processes, such as $^7\mathrm{Li} + {}^{12}\mathrm{C} \rightarrow {}^7\mathrm{Be} + {}^{11}\mathrm{B} + n$. Such processes could be independent of elementary isovector excitations. In any case, target-dependent effects could complicate a comparison between ^{40}Ca and ^{12}C.

In order to help clarify the situation, we have performed the (^{7}Li, ^{7}Beγ) reaction on the same target nucleus as used in the inelastic proton scattering experiment. The aim of the experiment was to see whether or not one observes a spin transfer enhancement at high excitation energy with the (^{7}Li, ^{7}Beγ) reaction on calcium. If so, given that one observes no such enhancement with a carbon target, one may conclude that target-dependent effects between ^{12}C and ^{40}Ca are an important consideration. If, on the other hand, there were no enhancement for calcium, then it would be clear that the details of the reaction mechanism complicate a comparison of the ($\vec{p},\vec{p}'$) and (^{7}Li, ^{7}Beγ) results. We have also used a higher bombarding energy than used by Nakayama *et al.*, which leads to the linear momentum transfer, q, being more closely matched to that of the small to medium angle ($\vec{p},\vec{p}'$) data, where the spin transfer enhancement was most pronounced.

Nakayama *et al.* [3,6] have demonstrated that the (^{7}Li,

*Present address: GANIL, B.P. 5027, 14021 Caen Cedex, France.
†Present address: Department of Mechanical Engineering, Texas A&M University, College Station, Texas 77843.
‡Present address: Institut de Physique Nucléaire, IN$_2$P$_3$-CNRS, 91406 Orsay Cedex, France.
§Present address: Ford Research Laboratory, MD#3429, 2000 Rotunda Drive, Dearborn, Michigan 48121.
‖Present and permanent address: Institut de Physique Nucléaire, IN$_2$P$_3$-CNRS, 91406 Orsay Cedex, France.

^{7}Be) charge exchange reaction can be used to separate $\Delta S=0$ and $\Delta S=1$ transitions through the coincidence measurement of the γ rays from the deexcitation of the 430 keV state of ^{7}Be. Whereas the transition to the ground state of ^{7}Be, $3/2^{-}\rightarrow 3/2^{-}$, is a mixture of nonspin transfer (Fermi) and spin transfer (Gamow-Teller) contributions, the transition to the 430 keV excited state of ^{7}Be, $3/2^{-}\rightarrow 1/2^{-}$, is pure spin transfer. Using known spectroscopic information from β-decay data [7], the nonspin transfer and spin transfer cross sections can be extracted from

$$\sigma(\Delta S=0)=\sigma(^{7}\mathrm{Be}_{0})-\sigma(^{7}\mathrm{Be}_{1})/0.72, \quad (1)$$

$$\sigma(\Delta S=1)=\sigma(^{7}\mathrm{Be}_{1})/1.11, \quad (2)$$

where $\sigma(^{7}\mathrm{Be}_{1})$ is the cross section for the coincidences (corrected for the γ-ray efficiency), and $\sigma(^{7}\mathrm{Be}_{0})$ is the cross section for the singles with the coincidences subtracted. This technique has also recently been applied by Janecke *et al.* [8] to study giant resonances.

It will often be convenient to refer to the corresponding excitation in the ^{40}Ca target, as if one had performed an inelastic scattering experiment. Excitation energies in the residual nucleus, ^{40}K, correspond to an equivalent excitation in the ^{40}Ca target after the Coulomb displacement energy of 7.7 MeV [9] is added.

The paper is organized as follows. After a section giving experimental details, we discuss the ^{40}Ca(^{7}Li, ^{7}Be)^{40}K singles spectrum, concentrating on the characteristics of two broad resonances which are observed. Next the technique for the γ-coincidence analysis is described, followed by an examination of the extracted spin transfer strength in ^{12}C and ^{40}Ca. The concluding section includes a brief discussion on the potential for further studies with the (^{7}Li, ^{7}Beγ) reaction on targets heavier than ^{40}Ca.

II. EXPERIMENTAL DETAILS

An $E/A = 70.4$ MeV ^{7}Li beam from the K1200 cyclotron at the National Superconducting Cyclotron Laboratory was used to bombard targets of ^{nat}C (3.1 mg/cm^{2}), Mylar ($C_5H_4O_2$, 0.83 mg/cm^{2}), and ^{nat}Ca (10.4 mg/cm^{2}). Scattered ^{7}Be particles were detected by the A1200 magnetic analyzer [10] operated as a 0° spectrometer, with the target at what is normally the second dispersive image. The momentum dispersion in this mode of operation is roughly 1.6 cm/% ($\delta p/p$). The maximum angle accepted in the laboratory frame was approximately 1.6°. An electrically isolated plate was placed on the high-rigidity side between the two dipoles of the spectrometer to intercept the ^{7}Li beam. Although the efficiency of charge collection by this plate was not determined (and hence we do not quote absolute cross sections), the integrated current could be used to compare relative reaction yields measured at the same magnetic field.

At the focal plane, a 7-cm long, 1-mm thick silicon position-sensitive detector (PSD) measured the particle rigidity. The energy-loss signal from the PSD together with the light output from a backing plastic scintillator was used for particle identification. A timing signal from the scintillator was used to trigger the acquisition system and was the time reference for the gamma-ray coincidences. A two-dimensional (XY) position-sensitive cathode readout drift chamber (CRDC), was mounted close to the silicon detector and another one mounted 30 cm in front of it. These two CRDC's were used to measure the angles of particles at the focal plane event by event. The readout of signals is by pads along the edges of these counters; they have no wires in the active area. No improvement to the energy resolution of the spectra could be made from angular correction terms with the CRDC's (implying that any spectrometer abberations were insignificant), and no corrections to the PSD position spectra were applied in the final pass through the analysis.

The energy resolution was approximately 1.5 MeV, which includes a linear contribution from the unresolved 430 keV doublet. The ^{40}Ca(^{7}Li, ^{7}Be)^{40}K focal plane spectrum was calibrated in energy by measuring the reaction on a Mylar target leading to known states in ^{12}B and ^{16}N, at the same magnetic field setting. Because of the more negative Q value, the reaction on the ^{nat}C target was measured at a lower field setting in order to obtain the high excitation region of the spectrum.

The calcium target was prepared and transported to the chamber with care to avoid oxidation. It was rolled under an argon atmosphere and then rinsed and coated with hexane. The target chamber was prepared by pumping to a high vacuum and then backfilling with argon. As soon as the target was placed in the ladder, the chamber was again pumped to high vacuum. The surface of the target appeared metallic and showed no sign of deterioration throughout the experiment. Despite these precautions, a considerable yield is observed from the reaction on hydrogen on the target relative to that for calcium (see the solid histogram in Fig. 1). The apparent yield of this contamination by hydrogen is greatly enhanced by the center-of-mass to laboratory transformation, together with a large cross section for H(^{7}Li, ^{7}Be)n. By comparing the yield of the hydrogen peak with that from the Mylar target, normalized by the charge collected on the beam-catching plate, we estimate that the amount of hydrogen on the calcium target was about 5 μg/cm^{2}. The likely sources of this hydrogen are from unevaporated hexane solvent or from incompletely removed mineral oil after the rolling process, rather than from oxidation through contact with air followed by absorption of water. The dotted histogram in Fig. 1 is the singles spectrum from the Mylar target, scaled to match the hydrogen peak from the calcium target. If the contamination were from hexane or oil residue, the carbon yield from the scaled Mylar spectrum would be an overestimation of the background at high excitation energies, since the chemical ratio C:H for hexane is 6:14 and that for common oils is roughly 1:2, compared to 5:4 for Mylar. Furthermore, judging by the few counts in the ^{16}N ground state and by the overall resemblance of the Mylar spectrum to that for the carbon target (not shown), the yield from oxygen in the Mylar target appears to be small. Thus we conclude that the possible interference from contaminants in the high excitation energy region of the calcium target is insignificant for our purposes. The tail of the hydrogen peak does obscure the ^{40}K ground state region. However, this region was not of direct interest in the present work.

An array of ten (3×3)-cm^{2} CsI scintillators, read by photomultipliers, was arranged around the target at a distance of approximately 5 cm. Stacks of absorbers, consisting

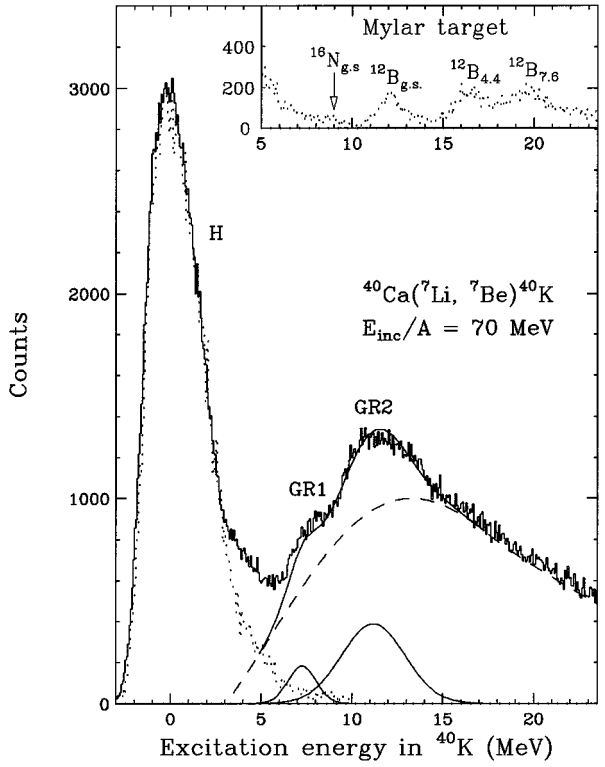

FIG. 1. Focal plane singles energy spectrum for the (^{7}Li, ^{7}Be) reaction on ^{40}Ca (solid line). The large peak labeled ''*H*'' arises from the ^{1}H(^{7}Li,^{7}Be)*n* reaction on hydrogen in the target. The dotted histogram in the main figure and in the inset is the spectrum for the reaction on the Mylar target, scaled in height to match the hydrogen peak with that for the calcium target. States in ^{12}B and ^{16}N from the Mylar target are indicated in the inset. In the main figure, the smooth dashed curve shows the assumed shape of the underlying continuum. The fitted Gaussians to the resonances labeled GR1 and GR2 are described in the text.

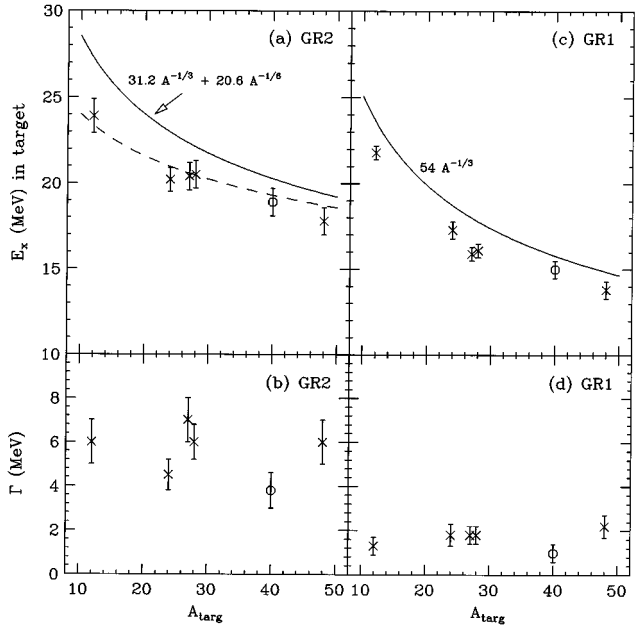

FIG. 2. The crosses show the measured excitation energies and widths of the resonances identified in Ref. [11] as the GDR [(a) and (b)] and IVOR [(c) and (d)], plotted as a function of target mass. The circles are the results for the resonances GR2 [(a) and (b)] and GR1 [(c) and (d)] obtained in the present work. Note that the present work indicates that GR1 is more likely to be a collective 2^- resonance than the IVOR. The curves are global predictions for the trends of the excitation energies of the GDR [17,16] and IVOR [18] described in the text. All excitation energies are expressed relative to that for the target nucleus.

of 1-mm each of aluminium, copper, and lead, were attached to the front of the scintillators to absorb x rays and low-energy γ rays. These absorbers are estimated to have attenuated the γ rays of interest by no more than 30%. The absolute efficiency of the CsI detectors was determined on line by reference to a transition of known strength, as described in Sec. III B. The CsI detectors and associated amplifiers were calibrated both before and after the beam time with ^{60}Co and ^{137}Cs sources. Although the gains of some of the CsI detectors were changed from the carbon target runs to the calcium target runs, which necessitated different gates between these runs, the Doppler-shifted 430-keV gamma ray was readily identified in the CsI spectra.

III. DATA ANALYSIS

A. Resonances in ^{40}Ca(^{7}Li, ^{7}Be)^{40}K singles spectrum

In the ^{40}Ca(^{7}Li, ^{7}Be)^{40}K singles spectrum (solid line in Fig. 1) we observe two resonancelike features: a small enhancement at roughly 7 MeV excitation energy in ^{40}K, which is labeled GR1, and a broad bump centered at roughly 11 MeV excitation energy in ^{40}K, labeled GR2. An addition of the Coulomb displacement energy gives the equivalent excitation in ^{40}Ca of GR1 and GR2 as roughly 15 MeV and 19 MeV, respectively.

We have made a double-Gaussian fit to the region of the two resonances, after subtracting a smooth background of an assumed continuum (see Fig. 1). The centroid (in the equivalent ^{40}Ca system) of the fitted Gaussian to GR1 is 15.0 ± 0.5 MeV with a full width at half maximum (FWHM) of 1.8 ± 0.4 MeV (the errors are estimated from the uncertainty in the peak fitting procedure). The centroid for GR2 is 18.9 ± 0.8 MeV with a FWHM of 4.1 ± 0.8 MeV. To facilitate comparison of the widths with other work, we subtract the experimental resolution (1.5 MeV) in quadrature from the FWHM, and obtain $\Gamma_{GR1}=0.98\pm0.4$ MeV and $\Gamma_{GR2}=3.8\pm0.8$ MeV. The centroids and corrected widths are plotted in Fig. 2 together with results from the analysis of the (^{7}Li, ^{7}Be) reaction on target nuclei ranging from ^{12}C to ^{48}Ti [11]. The excitation energies for GR1 and GR2 are seen to be consistent with the trends of similar resonances which were identified in the work of Ref. [11] as the isovector octupole resonances (IVOR) and giant dipole resonances (GDR), respectively. This identification was based mainly on comparison of their angular distributions with distorted wave Born approximation (DWBA) calculations. The width of the resonances that we observe are also consistent with the systematics from the earlier work. One observes large fluctuations in the values of the widths of GR2 in Fig. 2, leading one to suppose that this quantity is particularly sensitive to the assumed shape of the background continuum.

The resonance GR2 is evidently the well-known $T_>$ analogue of the GDR in ^{40}Ca. This has previously been observed in the (^{13}C, ^{13}N) reaction [12] and also in the (n,p)

reaction [13,14] on the same target.

The identity of resonance GR1 is not obvious from the singles spectrum alone. Although Nakayama *et al.* [11] have assigned the IVOR to the resonance which they observe, a collective 2^- state in this region has also been reported in (p,n) and $(^3\mathrm{He},t)$ studies [15]. The angular distributions measured in Ref. [11] were better reproduced by DWBA calculations with $\Delta J^\pi = 3^-$ than those with $\Delta J^\pi = 2^-$. Despite this, as will be shown in Sec. III B 2, we find almost no $\Delta S = 0$ strength in this excitation energy region, which suggests that, on the contrary, the resonance is more likely to be 2^- than 3^-.

The centroid energy of the GDR relative to the target nucleus excitation has been parameterized by [16,17]

$$E_{\mathrm{GDR}} = 31.2A^{-1/3} + 20.6A^{-1/6}\ \mathrm{MeV}. \tag{3}$$

This is plotted as the solid line in Fig. 2(a), and while giving a good account of the general trend of the data, is seen to predict values several MeV higher than the experimental ones. A three-parameter relation from Ref. [17] that provides a transition from an $A^{-1/6}$ power law at low mass numbers to an $A^{-1/3}$ power law at high mass numbers is

$$E_{\mathrm{GDR}} = 77.9A^{-1/3}(1 - e^{-A/A_0}) + 34.5A^{-1/6}e^{-A/A_0}\ \mathrm{MeV},$$

where $A_0 = 238$. This is plotted as the dashed line in Fig. 2(a) and is seen to be in much better agreement with the data than the two-parameter relation.

Although it now appears questionable that the resonance GR1 is the IVOR, we show in Fig. 2(c) a prediction by Nishimura *et al.* [18] of the centroid energy of the IVOR:

$$E_{\mathrm{IVOR}} = 54A^{-1/3}\ \mathrm{MeV}.$$

This predicts values higher than the experimental ones, while giving the correct general trend. However, as we have seen a similar disagreement for the simple parametrization of the GDR energy [Eq. (3)], we are unable to draw any firm conclusions from this observation.

B. Coincidence analysis

The Doppler-shifted 430 keV γ rays were identified for each CsI detector from plots of E_γ vs T_γ in coincidence with ^{7}Be. Gates were set on the prompt coincidence time peaks, and also on random time peaks (which were less than 3% of the prompt) for later subtraction.

Figure 3 shows a selection of projected γ-energy spectra for CsI detectors at different angles, obtained with the calcium target. The 430-keV peak is prominent in all detectors. Most of the counts on the low-energy side of the peak may be attributed to escaping Compton-scattered photons. While there were few counts on the high-energy side of the peak in the case of the carbon target, this was not the case for the calcium target. This background presumably arises from target deexcitations, the exact shape and magnitude of which would be complicated to predict because of the high density of states in ^{40}K and the likelihood of cascading transitions. To a certain extent one can see what the background might

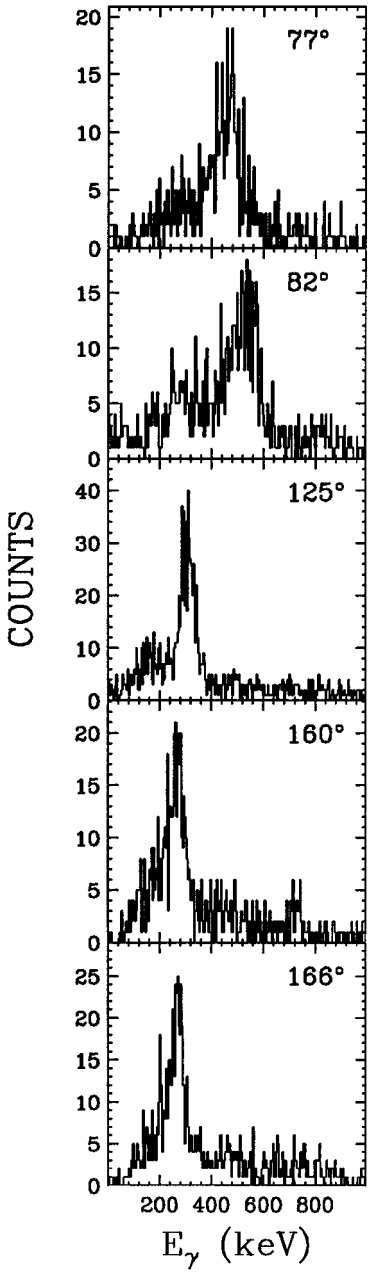

FIG. 3. Gamma-ray energy spectra gated on true coincidences with ^{7}Be in the focal plane. Spectra from five sample CsI detectors at different angles to the beam are shown (with the convention that angles less than 90° are forward with respect to the beam). Note that the ^{7}Be coincidence includes that for the dominant hydrogen peak. Thus the relative amount of target deexcitation background observed in these spectra lies between the 21% for the high excitation Ca region and the 7% for the hydrogen region quoted in the text.

be as the Doppler-shifted 430-keV peaks move along the laboratory frame from detector to detector (Fig. 3). From the number of counts in regions of the same width as the 430-keV gate, the γ background in coincidence with ^{7}Be particles in the focal plane, but *excluding* the region of the hydrogen peak, was estimated as 21 ± 5% of the 430-keV peak. As might be expected, the background-to-peak ratio in coincidence *with* the region of the hydrogen peak, where

there are few deexcitation γ rays, is much reduced, amounting to roughly 7%.

The CsI photopeak efficiency, which is required in order to normalize the $^7\mathrm{Be}_1$ spectrum, was estimated from the number of counts in the $^{12}\mathrm{B}_{\mathrm{g.s.}}$ (1^+) peak in the coincidence spectrum relative to the corresponding number in the singles spectrum. This ratio, for a pure $\Delta S=1$ transition, should equal 0.42 [3]. The contribution from the unresolved 0.95 MeV (2^+) state was estimated from a multiple Gaussian fit to the low-lying region of the ^{12}B spectrum, with centroids held fixed at the known energy spacings and widths made equal to that observed for the closely spaced $2^-/4^-$ doublet at 4.4 MeV. As a result, the absolute CsI efficiency was deduced to be 1.48×10^{-2}. Relative cross sections for σ ($^7\mathrm{Be}_1$) and $\sigma(^7\mathrm{Be}_0)$ were then made, and hence, from Eqs. (1) and (2), $\sigma(\Delta S=0)$ and $\sigma(\Delta S=1)$. Finally, the ''relative strength of spin transfer excitations,'' defined in Ref. [3] as

$$P_{\mathrm{sf}}=\frac{\sigma(\Delta S=1)}{\sigma(\Delta S=0)+\sigma(\Delta S=1)},$$

was calculated. For unnatural parity transitions the value of P_{sf} should be unity. In order to reduce statistical scatter, the data were rebinned into excitation energy bins of 0.3 MeV.

1. Spin transfer strength for the ^{12}C target

The spin strength analysis for the ^{12}C target is shown in Fig. 4, plotted in a similar way to the presentations in [3,4]. For ease of comparison with [3,4], the left-hand scale of Fig. 4(c) is the ''spin-flip ratio,'' $R=^7\mathrm{Be}_1/^7\mathrm{Be}_0$. Although the present experiment does not completely resolve the low-lying states in ^{12}B, which will lead to some crossmixing of $\Delta S=0$ and $\Delta S=1$ strength, we have attempted to analyze selected excitation energy bins which should have dominant contributions from the same states analyzed in Ref. [3] where the states were completely resolved. Presumably because of the lack of resolution, the values of P_{sf} at the locations of the ground (1^+) and 1.67 MeV (2^-) states are somewhat below the expected value of 1.0, although the values of P_{sf} at the excitation energies of the close-by 0.95 MeV (2^+) and 2.62 MeV (1^-) states are consistent with 0.5 as found in the previous work. Again, the value of P_{sf} for the $2^-/4^-$ doublet at $E_x=4.4$ MeV, which should be purely spin transfer, is lower than unity, but still significantly higher than that for the parts of the spectrum with contributions from $\Delta S=0$, such as the broad isovector dipole resonances [3,19,17] centered at $E_x=7.6$ MeV.

Importantly, the spin transfer analysis of the high excitation continuum, where the energy resolution is not critical, gives $P_{\mathrm{sf}}=0.44\pm0.03$, which agrees with the fundamental conclusion of Refs. [3,4] that comparable $\Delta S=0$ and $\Delta S=1$ strength is found at high excitation energy.

2. Spin transfer strength for the ^{40}Ca target

The spin strength analysis for the ^{40}Ca target is shown in Fig. 5. Beyond the region of the hydrogen peak, one sees a dramatic rise in the value of P_{sf} at around 6 MeV excitation energy. This appears to be a result of the almost complete cancellation of the singles and coincidence yield to give negligible $\Delta S=0$ strength at this excitation energy [Fig. 5(a)]. The origin of the cancellation is not known. However, the absence of $\Delta S=0$ strength includes the region of the resonance GR1 observed in the singles spectrum. The lack of $\Delta S=0$ strength suggests the assignment of 2^- rather than 3^- for this resonance, as discussed in Sec. III A.

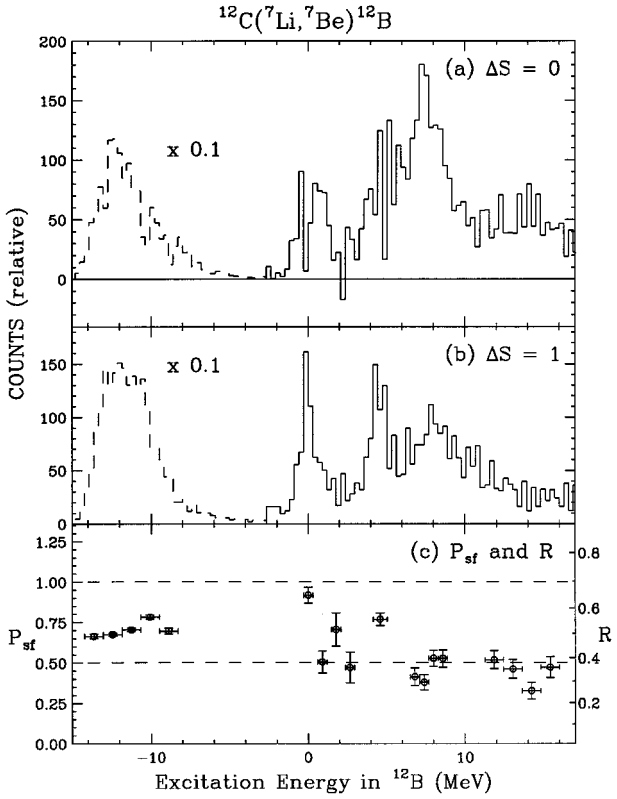

FIG. 4. Extracted energy spectra for (^{7}Li, ^{7}Be) on ^{12}C at $\theta_L\approx0°$ and $E/A=70$ MeV for the (a) nonspin transfer and (b) spin transfer channels, and (c) the relative strength of spin excitations. The yield in the region of the hydrogen peak has been scaled by one-tenth. The horizontal bars on the data points in (c) indicate the range of averaging over excitation energy. The vertical bars represent statistical errors only.

One observes considerable $\Delta S=0$ strength from roughly 9 MeV to 13 MeV excitation energy in ^{40}K, which covers the region of the GDR analogue seen in the singles spectrum. The resulting mean value of P_{sf} in the region of the analogue GDR, 0.41, is the smallest observed in the spectrum. The GDR is well known to be mainly nonspin transfer (see, e.g., [19,3]). Above 13 MeV excitation in ^{40}K (which would be equivalent to 20.7 MeV excitation in the ^{40}Ca analogue), the $\Delta S=0$ strength begins to fall and there is a corresponding small increase in P_{sf}. The average value of P_{sf} is 0.54 ± 0.02 from 17 to 22 MeV excitation in ^{40}K (corresponding to roughly 25 to 30 MeV excitation in ^{40}Ca). Thus it appears that the high excitation region for the ^{40}Ca target does have more $\Delta S=1$ strength than that for the ^{12}C target, being separated by the statistical errors by more than two standard deviations (although one has also to consider systematic errors). It has to be said on the other hand, that we do not observe such an outstanding rise in spin strength with increasing excitation energy as seen in the $(\vec{p},\vec{p}\,')$ experi-

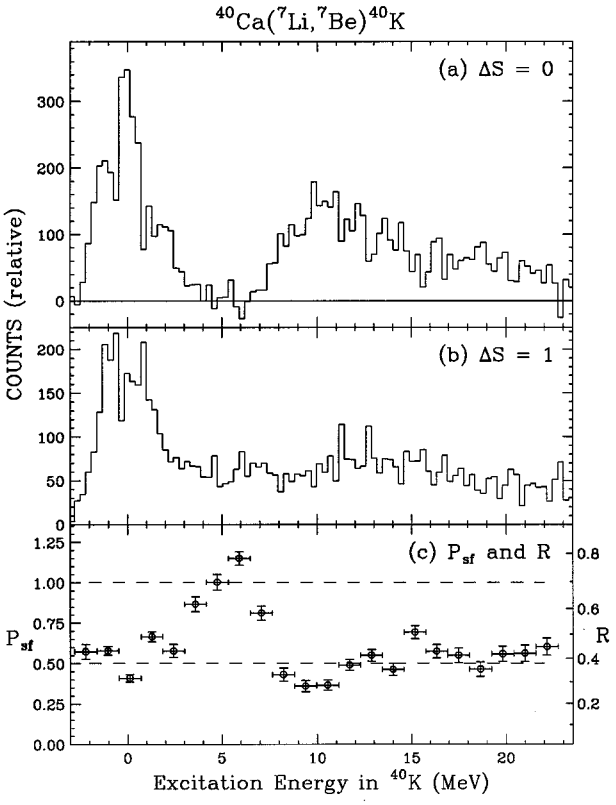

FIG. 5. Extracted energy spectra for (^{7}Li, ^{7}Be) on ^{40}Ca at $\theta_L \approx 0°$ and $E/A = 70$ MeV for the (a) nonspin transfer and (b) spin transfer channels, and (c) the relative strength of spin excitations. The horizontal bars on the data points in (c) indicate the range of averaging over excitation energy. The vertical bars represent statistical errors only.

ment, both in terms of the absolute value of P_{sf} and relative to the lower excitation portion of the spectrum.

IV. DISCUSSION AND CONCLUSIONS

The most probable systematic uncertainty in P_{sf} between the carbon and calcium target measurements comes from the lack of ''cleanliness'' of the 430 keV γ-ray gate. First, because of the previously mentioned gain changes in some of the CsI detectors, the gates for the calcium target were not always the same as those for the carbon target. Second, the γ-ray background which was subtracted from the coincidence spectrum for calcium is uncertain to about 5% (the background for the carbon target was essentially negligible). This gives a systematic uncertainty of somewhat less than 10% in P_{sf}, since both the $^{7}\mathrm{Be}_0$ and $^{7}\mathrm{Be}_1$ yield are affected.

A comparison between the carbon and calcium targets of the P_{sf} values obtained for the hydrogen peak may indicate the size and sense of any systematic errors. Unfortunately, the need to avoid the underlying ground-state region of ^{40}K prevents a straightforward comparison. Nevertheless the averages of 0.70 ± 0.01 for the carbon target and 0.60 ± 0.02 (excluding $E_x \approx 0$ MeV) for the calcium target, suggest that too much background has been subtracted from the γ-coincidence spectrum of the latter. If the background were indeed oversubtracted, then the actual difference in the spin transfer strength at high excitation between the calcium and carbon targets would be more pronounced. To be sure of the precise background at the high excitation end of the spectrum, one would need to investigate any possible correlation of the gamma-ray background from target deexcitation with excitation energy. The present experiment does not have sufficiently good statistics for this. Even in the worst case, the systematic errors appear to be smaller than the observed difference in the P_{sf} values, and they act in a sense that the effect would be larger if they were accounted for properly. However, the main conclusion is that there is no *significant* increase in spin strength compared to that observed in the $(\vec{p},\vec{p}')$ data, since the value for P_{sf} we obtain is close to one-half.

The issue of systematic uncertainty arising from background γ rays in the present experiment raises the question of the general applicability of the (^{7}Li, ^{7}Beγ) reaction. The technique in the past has been limited to rather light targets: The pioneering works of Nakayama *et al.* used ^{12}C [3] and ^{28}Si [4] targets. Janecke *et al.*, while having applied the technique to ^{6}Li, was not able to obtain spin transfer ratios for targets of ^{90}Zr, ^{120}Sn, and ^{208}Pb ''because of interference with γ rays from the deexcitation of the residual nuclei'' [8]. This limitation may be overcome by a new multi-segmented gamma detector [20] which has been constructed for use at RCNP, Osaka University. This detector will allow not only a higher beam intensity because of the reduced singles count rate in the individual detectors, but will also limit the Doppler broadening of the 430-keV peak.

In summary, following the systematic study of Nakayama *et al.* [11], the (^{7}Li, ^{7}Be) reaction has again been shown to be a useful tool to investigate isovector giant resonances. The γ-coincidence technique has been applied to measure the spin transfer strength, particularly in the high excitation continuum. Although the data indicate that more spin transfer strength lies in the continuum for the calcium target than for carbon, which may partially account for the discrepancy between the ^{12}C(^{7}Li, ^{7}Beγ) and the ^{40}Ca$(\vec{p},\vec{p}')$ experiments, it appears that the greater part of the discrepancy must be explained by differing features of the light-ion and heavy-ion reaction mechanisms. Finally, we conclude that if the (^{7}Li, ^{7}Beγ) technique is to be successfully applied to targets significantly heavier than ^{40}Ca (for example, to ^{90}Zr), a finely segmented γ detector should be used to ameliorate the interference of target deexcitation γ rays.

ACKNOWLEDGMENTS

J.S.W. would like to thank the staff at the Institut de Physique Nucléaire d'Orsay for the generous hospitality shown during his visit. We are indebted to S. Nakayama for helpful communications, to J. Jänecke for a comment regarding the widths of giant resonances, and to N.A. Orr for a careful reading of the manuscript. Financial support from the Centre International des Etudiants et Stagiaires, the Centre National de la Recherche Scientifique, and the U.S. National Science Foundation under Grant No. PHY92-14922 is gratefully acknowledged.

[1] C. Glashausser, K. Jones, F.T. Baker, L. Bimbot, H. Esbensen, R.W. Fergerson, A. Green, S. Nanda, and R.D. Smith, Phys. Rev. Lett. **58**, 2404 (1987).

[2] H. Esbensen and G. Bertsch, Ann. Phys. **157**, 226 (1984); Phys. Rev. C **34**, 1419 (1986).

[3] S. Nakayama, T. Yamagata, M. Tanaka, M. Inoue, K. Yuasa, T. Itahashi, H. Ogata, N. Koori, and K. Shima, Phys. Rev. Lett. **67**, 1082 (1991).

[4] S. Nakayama, T. Yamagata, M. Tanaka, M. Inoue, K. Yuasa, T. Itahashi, H. Ogata, N. Koori, K. Shima, and M.B. Greenfield, Nucl. Phys. **A538**, 627c (1992).

[5] I. Lhenry in *The Groningen Conference on Giant Resonances*, edited by J. C. Bacelar, M. N. Harakeh, and O. Scholten [Nucl. Phys. **A599**, 245c (1996)].

[6] S. Nakayama, T. Yamagata, M. Tanaka, M. Inoue, K. Yuasa, T. Itahashi, H. Ogata, N. Koori, and K. Shima, Nucl. Instrum. Methods A **302**, 472 (1991).

[7] F. Ajzenberg-Selove, Nucl. Phys. **A490** 1 (1988).

[8] J. Janecke, T. Annakkage, G.P.A. Berg, J.A. Brown, G. Crawley, S. Danczyk, M. Fujiwara, D.J. Mercer, K. Pham, D.A. Roberts, J. Stasko, J.S. Winfield, and G.H. Yoo, in *The Groninger Conference on Giant Resonances*, edited by J. C. Bacelar, M. N. Harakeh, and O. Scholten [Nucl. Phys. **A599** 191c (1996)].

[9] W.J. Courtney and D.J. Fox, At. Data Nucl. Data Tables **15**, 142 (1975).

[10] B.M. Sherrill, D.J. Morrissey, J.A. Nolen, Jr., and J.A. Winger, Nucl. Instrum. Methods B **56/57**, 1106 (1991).

[11] S. Nakayama, T. Yamagata, K. Yuasa, M. Tanaka, M. Inoue, T. Itahashi, and H. Ogata, Phys. Lett. B **195**, 316 (1987).

[12] C. Bérat, M. Buenerd, J. Chauvin, J.Y. Hostachy, D. Lebrun, P. Martin, J. Barrette, B. Berthier, B. Fernandez, A. Miczaika, W. Mittig, E. Stilliaris, W. von Oertzen, H. Lenske, and H.H. Wolter, Phys. Lett. B **218**, 299 (1989).

[13] C.M. Castaneda, J.L. Romero, F.P. Brady, J.R. Drummond, T.D. Ford, and B. McEachern, in *Neutron-Nucleus Collisions*: *A Probe of Nuclear Structure*, edited by J. Rapaport, R. W. Finlay, S. M. Grimes, and F. S. Dietrich, AIP Conf. Proc. No. 124 (AIP, New York, 1985), p. 143.

[14] J. Rapaport, in *Spin and Isospin in Nuclear Interactions*, edited by S.W. Wissink, C.D. Goodman, and G.E. Walker (Plenum, New York, 1991), p. 442; B.K. Park, J. Rapaport, J.L. Ullman, A.G. Ling, D.S. Sorenson, F.P. Brady, J.L. Romero, C.R. Howell, W. Tornow, and C.T. Rönnqvist, Phys. Rev. C **45**, 1791 (1992).

[15] D.J. Horen, C.D. Goodman, D.E. Bainum, C.C. Foster, C. Gaarde, C.A. Goulding, M.B. Greenfield, J. Rapaport, T.N. Taddeucci, E. Sugarbaker, T. Masterson, S.M. Austin, A. Galonsky, and W. Sterrenburg, Phys. Lett. **99B**, 383 (1981); S.Y. van der Werf, S. Brandenburg, A.G. Drentje, P. Grasdijk, M.B. Greenfield, M.N. Harakeh, W. Segeth, W.A. Sterrenburg, and A. van der Woude, J. Phys. (Paris) Colloq. **45**, C4-471 (1984).

[16] J.J. Gaardhøje, Annu. Rev. Nucl. Sci. **42**, 483 (1992).

[17] B.L. Berman and S.C. Fultz, Rev. Mod. Phys. **47**, 713 (1975).

[18] M. Nishimura, M. Fujiwara, and S. Nishizaki, Phys. Lett. B **190**, 11 (1987).

[19] C. Gaarde, J.S. Larsen, H. Sagawa, N. Ohtsuka, J. Rapaport, T.N. Taddeucci, C.D. Goodman, C.C. Foster, C.A. Goulding, D. Horen, T. Masterson, and E. Sugarbaker, Nucl. Phys. **A422**, 189 (1984).

[20] S. Nakayama, in *The Tours Symposium on Nuclear Physics II*, edited by H. Utsunomiya, M. Ohta, J. Galin, and G. Münzenberg (World Scientific, Singapore, 1994), p. 542; S. Nakayama, T. Iwawaki, N. Koori, T. Yamagata, and M. Tanaka, RCNP report, Osaka University, 1994.